A Natural Virucidal and Microbicidal Spray Based on Polyphenol-Iron Sols

Sang Yeong Han,‡[1] Gyeongwon Yun,‡[1] Hyeon-Min Cha,[2][3] Myoung Kyu Lee,[2] Hojae Lee,[5] Eunhye K. Kang,[1] Seok-Pyo Hong,[1] Kirsty A. Teahan,[4] Minjeong Park,[6] Hansol Hwang,[6] Seung Seo Lee,[4] Meehyein Kim,[2][3] and Insung S. Choi[1]**

[1] Department of Chemistry, KAIST, Daejeon 34141, Korea

[2] Infectious Diseases Therapeutic Research Center, KRICT, Daejeon 34114, Korea

[3] Graduate School of New Drug Discovery and Development, Chungnam National University, Daejeon 34134, Korea

[4] School of Chemistry and Institute for Life Sciences, Highfield Campus, University of Southampton, Southampton SO17 1BJ, United Kingdom

[5] Department of Chemistry, Hallym University, Chuncheon 24252, Korea

[6] Hansol RootOne, Inc., 165 Myeoncheon-ro, Dangjin 31803, Korea

*Email: mkim@krict.re.kr; ischoi@kaist.ac.kr

KEYWORDS. metal-phenolic sol, virucidal, microbicidal, polyphenols, spraying

ABSTRACT

Numerous disinfection methods have been developed to reduce the transmission of infectious diseases that threaten human health. However, it still remains elusively challenging to develop eco-friendly and cost-effective methods that deactivate a wide range of pathogens, from viruses to bacteria and fungi, without doing any harm to humans, or the environment. Herein we report a natural spraying protocol, based on a water-dispersible supramolecular sol of nature-derived tannic acid and Fe^{3+}, which is easy-to-use and low-cost. Our formulation effectively deactivates viruses (influenza A viruses, SARS-CoV-2, and human rhinovirus) as well as suppressing the growth and spread of pathogenic bacteria (*Escherichia coli*, *Salmonella typhimurium*, *Staphylococcus aureus*, and *Acinetobacter baumannii*) and fungi (*Pleurotus ostreatus* and *Trichophyton rubrum*). Its versatile applicability in a real-life setting is also demonstrated against microorganisms present on the surfaces of common household items (e.g., air filter membranes, disposable face masks, kitchen sinks, mobile phones, refrigerators, and toilet seats).

INTRODUCTION

The COVID-19 pandemic, caused by severe acute respiratory syndrome coronavirus 2 (SARS-CoV-2), has posed a public health threat devastating the global economy and altering our way of living with unprecedented social restrictions.[1-3] SARS-CoV-2 is transmitted primarily through direct or indirect exposure to infected secretion, such as saliva, respiratory droplets, or aerosols released during exhalation (e.g., breathing, speaking, singing, exercising, coughing, and sneezing).[4-6] The zoonotic RNA viruses, including SARS-CoV-2, Middle East respiratory syndrome (MERS)-CoV, and influenza A virus, are able to generate new variants consistently through genetic mutations, being recorded as major causative agents for the worst pandemics in history.[7,8] Although it is crucial to disinfect viruses typically found in the natural environment, to block their human-to-human or animal-to-human transmission, it has been challenging to develop disinfectants that inactivate wide families of viruses. More profoundly, it has been shown that not only viruses, but also fungi and bacteria, can remain in an active state for hours, or even days, on various surfaces present in our daily lives, such as doorknobs, kitchen sinks, face masks, and mobile phones, which act as a reservoir of pathogens, increasing transmission rates,[9,10] particularly problematic in the food industry or healthcare settings. Considering the diversity of pathogenic microorganisms, it is an ultimate goal to find a new class of disinfectants with long-lasting, broad-spectrum activity that is safe to use, with regards to human health and the environment.

Various disinfecting methods, using metal nanomaterials (e.g., copper, silver, and zinc oxide), polymers, chemicals, high temperature, UV irradiation, and gamma radiation, have been reported to prevent the spread of viral and microbial pathogens from contaminated surfaces.[11-17] Despite noticeable microbicidal activities, unavoidable shortcomings that are associated with health and

environmental concerns, duration time and/or cost, and the requirement of special apparatus have limited their widely accepted and daily implementation, particularly in some countries with inadequate resources and infrastructure.[18-21] Therefore, the development of cost-effective and eco-friendly methods that can readily and effectively deactivate pathogens (e.g., viruses, bacteria, and fungi) under ambient conditions is urgently needed.

Polyphenol-metal species, formed by coordination-driven self-assembly of multivalent metal ions (e.g., Fe^{3+}) and polyphenols, such as tannic acid (TA), have received prodigious attention in chemistry, biological and biomedical engineering, and materials science, due to their unique properties. These include material-independent-coating property and physicochemical stability, in addition to biocompatibility.[22-24] In the aspect of safety, TA and iron have been approved as cosmetic ingredients and food additives by the US Food and Drug Administration (FDA).[25] Moreover, TA, a naturally occurring compound found in plants, is a secondary metabolite that protects the plants from pathogens and UV radiation, and iron is deeply associated with antibacterial activities.[26-29] Considering the safety, economic efficiency, and microbicidal activity, TA and Fe^{3+} would have great promise as natural antimicrobial and virucidal materials for a wide range of pathogenic species.

Several coating methods for a TA-Fe^{3+} combination have so far been reported by us and others, including discrete, rust-assisted, biphasic, electrochemical, metal-phenolic sol (MPS), iron gall ink-inspired, and electrophoretic assembly.[30-50] However, these methods inevitably involve dip-coating (i.e., immersion-based) processes, in which a substrate is submerged in a TA-Fe^{3+} (or TA-Fe^{2+}) solution, making it challenging to coat bulk or fixed substrates and, of course, sanitize them. Furthermore, the uncontrolled rapid precipitation of TA-Fe^{3+} species in solution prevents its multiple use, which from an economic point of view is not ideal.[43] A spray-

based method has been reported,[51,52] but the process should be repeated in a layer-by-layer manner, and, more critically, requires the customized two-nozzle system that physically isolates the TA and Fe^{3+} solutions for prevention of precipitate formation. Its practical applications in a wide range of our daily lives are hence limited, although its antimicrobial effect has been demonstrated with mandarin oranges and strawberries in the development of edible coatings.[51] In this paper, we report a one-pot, one-nozzle, direct spraying method, based on water-dispersed TA-Fe^{3+}-MPS, which is used to disinfect viruses and microorganisms (Figure 1). Our nature-derived spraying formula effectively deactivates viruses (e.g., influenza A viruses, SARS-CoV-2, and human rhinovirus), bacteria (e.g., *Escherichia coli*, *Salmonella typhimurium*, *Staphylococcus aureus*, and *Acinetobacter baumannii*), and fungi (e.g., *Pleurotus ostreatus* and *Trichophyton rubrum*). Its microbicidal activity is also demonstrated against common microorganisms present in our daily life (e.g., air filter membranes, disposable face masks, kitchen sinks, mobile phones, refrigerators, and toilet seats).

EXPERIMENTAL SECTION

Materials. Tannic acid (TA, Sigma-Aldrich), iron(III) chloride hexahydrate ($FeCl_3 \cdot 6H_2O$, ≥98.0%, Sigma-Aldrich), L-ascorbic acid (≥99%, Sigma-Aldrich), sodium hydroxide (NaOH, 95.0%, Junsei), sodium chloride (NaCl, 99.5%, Daejung), hydrochloric acid (HCl, 35%, Junsei), ethanol (95%, Samchun Chemicals), acetone (99.5%, Samchun Chemicals), Luria-Bertani (LB) broth high salt (Duchefa Biochemistry), LB agar high salt (Duchefa Biochemistry), xylose-lysine-deoxycholate (XLD) agar (MBcell), tetrathionate broth supplement (MBcell), buffered peptone water (BPW, MBcell), tryptic soy broth (TBS, Sigma-Aldrich), tryptic soy agar (TSA,

Sigma-Aldrich), plate count agar (PCA, MBcell), Sabouraud dextrose (SD) broth (MBcell), SD agar (MBcell), 4',6-diamidno-2-phenylindole, dihydrochloride (DAPI, Invitrogen), serum-free minimal essential medium (MEM, Invitrogen), serum-free Dulbecco's modified Eagle's minimal essential medium (DMEM, HyClone), TPCK-treated trypsin (Sigma-Aldrich), goat anti-mouse IgG, IgM (H+L) secondary antibody, Alexa Fluor^{TM} 488 (Invitrogen), phosphate-buffered saline (PBS, pH 7.4, Welgene), crystal violet (Sigma-Aldrich), anti-spike antibody (Genetex), chicken eggs (Hansol RootOne), quartz plates (Merck), glass plates (Marienfeld), mushroom cultivation bottles (*Pleurotus ostreatus*, Dotori Agricultural Co., Ltd.), hand sprayers (Apollo), cotton fabric, poly(acrylic acid) (AC, ENGP), polystyrene (PS, ENGP), and polytetrafluoroethylene (PTFE, ENGP) were used as received. Al foil (99.997%), Cu foil (99.95%), Sn foil (99.8%), Ti foil (99.94%), and stainless steel (Fe:Cu:Ni; 70:19:11wt%) were purchased from Alfa Aesar. Si wafers (Sehyoung Wafertech) were used as received. Gold substrates were prepared by thermal deposition of Ti (5 nm) and Au (100 nm) onto the silicon wafers. Deionized (DI) water (18.3 MΩ·cm) from Milli-Q Direct 8 (Millipore) was used. TA-Fe^{3+}-MPS solutions were freshly prepared by mixing a TA solution (12 mM, DI water) with an equal volume of the Fe^{3+} solution (48 mM, DI water) at ambient temperature, prior to use.

Characterizations. The ellipsometric thickness was measured with an Elli-SE spectroscopic ellipsometer (Ellipso Technology). At least three independent points of each sample were measured, and average values (with at least 9 measurements) were recorded. Contact angle measurements were performed using a Phoenix 300 goniometer (Surface Electro Optics Co.) equipped with a video camera. The static contact angle of a 3-μL water droplet was measured at four different locations on each sample. Field-emission scanning electron microscopy (FE-SEM) imaging was performed with an Inspect F50 microscope (FEI) with an accelerating voltage of 10

kV, after sputter-coating with platinum. Atomic force microscopy (AFM) image was obtained with a NanoWizard 4 XP BioScience AFM (JPK). The AFM analysis was performed in the tapping mode using an HQ:NSC15/Al BS tip (MikroMasch). X-ray photoelectron spectroscopy (XPS) spectra were acquired with a Sigma Probe (Thermo VG Scientific), and UV-visible (UV-vis) absorption spectrum was acquired with a UV-2550 spectrophotometer (Shimadzu). The *L** values were measured with a TES-135A (TES Electrical Electronics Corp.). For the *L**values, at least twenty measurements were performed per sample, and the averaged values with standard deviations were reported. The formation of TA-Fe^{3+} particles in the spraying solution was characterized with a confocal laser scanning microscope (CLSM; LSM 700, Carl Zeiss) in the differential interference contrast (DIC) mode. At least 4 independent images of each sample were taken for the analysis. The optical density was measured at 600 nm with a UV-2550 Visible spectrophotometer (Shimadzu).

Virucidal Effects. *(1) Influenza viruses*: Influenza A viruses, PR8 (subtype: H1N1) and HK (subtype: H3N2), were prepared in serum-free MEM in the presence of TPCK-treated trypsin (2 μg mL^{-1}), being estimated at 2×10^6 PFU mL^{-1}. Each virus was incubated with an equal volume of TA-Fe^{3+}-MPS or MEM for 30 min at room temperature. When needed, their incubation time and temperature can be modified. After incubation, the virus suspensions were 10-fold serially diluted (from 10^0 to 10^{-9}) in the MEM with TPCK-treated trypsin, and 100 μL of the diluted samples were treated into MDCK cells, followed by seeding in 96-well plates at a density of 3×10^4 cells per well. As controls, mock-infected MDCK cells were cultured in the MEM with TPCK-treated trypsin or TA-Fe^{3+}-MPS. On day 3 after infection at 33 °C, the cells were fixed and stained with crystal violet for 1 h. Viable-cell percentage was determined by counting the number of stained wells from total 8 wells. *(2) SARS-CoV-2*: SARS-CoV-2 (hCoV-

19/Korea/KCDC06/2020), belonging to the clade S, was provided by the Korea Disease Control and Prevention Agency. The virus (10^6 PFU mL^{-1}) was incubated with an equal amount of culture medium or TA-Fe^{3+}-MPS for 30 min at room temperature. Their 10-fold serial dilutions in serum-free DMEM were treated to Vero 1 cells at 37 °C for 2 days. To count the infected-cell population, the cells were immuno-stained with an anti-spike protein antibody and Alexa Fluor 488-labeled goat anti-mouse IgG according to our previous report.[53] All experiments with SARS-CoV-2 have been conducted at a biosafety level 3 facility at KRICT. *(3) Human rhinovirus (HRV-14)*: the non-enveloped HRV-14 (10^5 PFU mL^{-1}) was mixed with DMEM or TA-Fe^{3+}-MPS as mentioned just above. Their serial dilutions were loaded onto H1 HeLa cells at 33 °C. After 3 days, the well number with virus-infected cells was counted by crystal violet staining. All $TCID_{50}$ values were determined by the Reed-Muench method.[54]

Bactericidal Effects. (1) *E. coli*: A single colony of *E. coli* (MG 1655) was isolated from an LB agar plate and cultivated in the LB broth liquid media for 18 h with shaking at 120 rpm at 37 °C. Prior to use, the *E. coli* cells were washed with an aqueous NaCl solution (150 mM). The E. coli suspension (optical density at 600 nm: 0.2) was serially diluted up to10^{-4}-fold with a NaCl solution (150 mM), and then 150 μL of the resulting suspension was spread on an LB agar plate. After 30 min of incubation at ambient temperature, the TA-Fe^{3+}-MPS spraying was performed five times on the LB agar plate. The plate was then incubated at 37 °C under static conditions for 24 h. (2) *S. typhimurium*: A single colony of *S. typhimurium* (ATCC 14028) was isolated from an XLD agar plate and cultivated in the BPW liquid media for 24 h with shaking at 120 rpm at 37 °C. After mixing 1 mL of BPW of the primary growth bacteria media with 10 mL of tetrathionate broth, the cells were incubated for 18 h with shaking at 37 °C and then washed with an aqueous NaCl solution (150 mM). The *S. typhimurium* suspension (optical density at 600 nm:

0.2) was serially diluted up to 10^{-5}-fold and the solution (150 μL) was spread on an XLD agar plate. After 30 min of incubation at ambient temperature, the TA-Fe^{3+}-MPS was sprayed on the agar plate five times. The plate was then incubated at 37 °C under static conditions for 24 h. (3) *S. aureus*: A single colony of the *S. aureus* (patient-derived USA 300) was isolated from an overnight grown TSA plate and inoculated in TSB liquid media. The culture was grown for 18 h with shaking at 120 rpm at 37 °C. The overnight culture was washed with 150-mM NaCl solution and serially diluted up to 10^{-4}-fold, and the adjusted suspension was spread on a TSA plate. After 30 min of incubation at ambient temperature, the TA-Fe^{3+}-MPS was sprayed on the plate five times, which was then incubated at 37 °C under static conditions for 24 h. (4) *A. baumannii*: The same procedure as that for *E. coli* was followed for the experiment with *A. baumannii* (patient-derived ATCC 17978) except the final suspension to be plated was prepared by 10^4-fold dilution of an overnight culture. Two controls were prepared in each experiment. The first was the sample sprayed with only water 5 times, and the second the sample without spraying. The bactericidal effects of the TA-Fe^{3+}-MPS spraying against respective bacteria were determined by the colony-forming unit (CFU) number per agar plate.

Fungicidal Effects. (1) *P. ostreatus*: The TA-Fe^{3+}-MPS spraying was performed to a mushroom cultivation bottle five times every morning (around 9 am), and the mushroom height was measured in the afternoon (around 5 pm). The mushroom growth was monitored for 1 week. Water spraying with tap water was used as a control. (2) *T. rubrum*: A colony of *T. rubrum* (ATCC 28188) was picked from a SD agar plate and cultivated in the SD broth liquid media for 24 h with shaking at 120 rpm at 30 °C. Before fungicidal testing, commercial shoe insoles were immersed in an SD broth solution for 30 min to supply nutrients for fungal growth. The *T. rubrum* suspension (1 mL) was spread on the shoe insoles, followed by 30 min of incubation at

ambient temperature. The TA-Fe^{3+}-MPS spraying, or water spraying (control) was performed on the shoe insoles five times every morning (around 10 am). The growth and spread of the moulds were characterized after two days of incubation at 30 °C under closed conditions.

Material Independency and Coating Durability. (1) *Contact angle measurement*: Prior to use, all of the substrates were cleaned with ethanol or DI water under sonication and dried under a stream of argon gas. The wettability of each sample was measured before and after five TA-Fe^{3+}-MPS sprayings. (2) *Durability*: The *L** (lightness) value of the cotton fabric was measured before and after five TA-Fe^{3+}-MPS sprayings. After spraying, the cotton fabric was washed with DI water (pH 7.5, adjusted with 1 M NaOH solution) and dried under ambient conditions. For the durability analysis, the *L** value of the cotton fabric was measured after washing with tap water and drying. For the egg experiment, chicken eggs were sprayed with TA-Fe^{3+}-MPS, immediately followed by washing with tap water and drying under ambient conditions. The coating-washing-drying cycle was repeated four times. (3) *Film thickness*: All of the solutions were freshly prepared for immediate use. The TA-Fe^{3+}-MPS spraying solution was prepared by mixing a TA solution (3, 6, 12, 24, or 48 mM) with an equal volume of the Fe^{3+} solution (6, 12, 24, 48, 96, or 192 mM) at ambient temperature. The distance between a hand sprayer and the gold substrate was fixed to be 5 cm. After five TA-Fe^{3+}-MPS sprayings, the substrate was washed with DI water (pH 7.5, adjusted with 1 M NaOH solution) to remove excess TA-Fe^{3+} complex and dried under a stream of argon. The film thickness was measured by spectroscopic ellipsometry.

Real-Life Applications. Microorganisms were sampled from the household surfaces, such as air filter membranes, toilet seats, kitchen sinks, refrigerators, disposable face masks, and mobile phones, with sterilized cotton swabs. The disposable face masks were used for 12 h in daily life,

and then microorganisms were collected from the used masks. The collected samples were immersed in a 0.85% NaCl solution (1 mL) under vigorous shaking for 10 min. The 10-fold diluted solution (150 μL) was spread on a PCA plate, and after 30 min of incubation at ambient temperature, the TA-Fe^{3+}-MPS spraying or water spraying (control) was performed five times on the PCA plate, followed by incubation at 37 °C under static conditions for 30 h. As real-life applications, the spraying was directly carried out on the toilet seat, kitchen sink, and mobile phone. After 1 h of storage under ambient conditions, each sample was taken from the sprayed surface with a sterilized cotton swab for analysis.

RESULTS AND DISCUSSION

Virucidal Activity. To assess the virucidal effect of our spraying solution, two different enveloped viruses, influenza A virus and SARS-CoV-2, and a non-enveloped one, human rhinovirus (HRV-14), were selected as models. HRV-14 causes milder symptoms through upper respiratory tract infections than SARS-CoV-2 and others, but its prevention and treatment are limited due to the absence of clinically approved vaccines or therapeutics.[55] Moreover, rhinovirus, belonging to the family *Picornaviridae*, has been regarded as resistant to both extremely acidic and basic conditions, heat, dryness, and most of the available disinfectants.[56-59]

Two subtypes of influenza A virus strains were used for the study: A/Puerto Rico/8/1934 (PR8; H1N1) and A/Hong Kong/8/1968 (HK; H3N2). They, at a titre of 2×10^6 plaque-forming unit (PFU) mL^{-1}, were incubated with an equal volume of TA-Fe^{3+}-MPS (final concentration: [TA] = 6 mM; [Fe^{3+}] = 24 mM) at room temperature for 30 min. Changes of viral infectivity were determined by a cytopathic effect-based median tissue culture infectious dose ($TCID_{50}$) assay, in which MDCK cells were infected with 10-fold serial dilutions (from 10^0 to 10^{-9}) of

mock-treated or TA-Fe^{3+}-MPS-treated virus samples. On day 3 post-infection, the crystal violet staining showed that the infectivity of both PR8 and HK disappeared after exposure to TA-Fe^{3+}-MPS (Figure 2a and Figure S1). Quantitatively, 30-min incubation with the TA-Fe^{3+}-MPS resulted in loss of viral infectivity by reducing plaque titres below the limit of detection (LOD), while their mock-treated PR8 and HK samples had $TCID_{50}$ values of 8.1 ± 0.5 log($TCID_{50}$ mL^{-1}) and 7.5 ± 0.6 log($TCID_{50}$ mL^{-1}), respectively. We further examined whether this disinfection efficacy was reproducible against another respiratory enveloped virus, SARS-CoV-2. Viral infectivity to Vero cells were compared in the absence or presence of TA-Fe^{3+}-MPS by the immunofluorescence-based assay, in which viral spike (S) protein was stained with its primary antibody and a fluorescently labelled secondary antibody. Notably, based on the fluorescence-positive cell population, it was observed that the titre of SARS-CoV-2 (7.2 ± 0.1 log($TCID_{50}$ mL^{-1})) drastically decreased below LOD in the presence of TA-Fe^{3+}-MPS (Figure 2b,c). The results suggested that the TA-Fe^{3+}-MPS formula led to at least 5-log reductions in the infectivity of influenza A virus and SARS-CoV-2. In addition, considering that the removal of non-enveloped viruses is more difficult than enveloped ones, we tested whether HRV-14 was sensitive to TA-Fe^{3+}-MPS. Following the same procedure used in the influenza A virus assay, $TCID_{50}$ values were measured after HRV-14 infection into H1 HeLa cells. It was observed that the virus at a titre of 6.1 ± 0.2 log($TCID_{50}$ mL^{-1}) completely lost its infectivity by TA-Fe^{3+}-MPS (Figure 2d and Figure S2). Taken together, our feasibility tests confirmed that TA-Fe^{3+}-MPS would be a ready-to-use, broad-spectrum virucidal agent that inactivates both enveloped and non-enveloped viruses.

Furthermore, we investigated how rapidly TA-Fe^{3+}-MPS achieved the viral clearance with PR8. PR8 was incubated with TA-Fe^{3+}-MPS for 10, 20, or 30 min at room temperature (Figure

2e), and it was demonstrated that viral titre was already decreased to a baseline level after only 10 min. This time course study demonstrated that its treatment rendered the virus at a TCID50 of approximately 7.5 log($TCID_{50}$ mL^{-1}) inactivated within 10 min. In addition to rapidity, for field application of a disinfectant, it is critical to assess its working temperature since viruses can circulate and remain active at variable outdoor thermal environments, such as heat and cold stresses. To evaluate temperature dependency of the cytopathic-effect reduction, PR8 was treated with TA-Fe^{3+}-MPS for 30 min at different temperatures, 4, 25, and 37 °C (Figure 2f). Comparative analysis, by measuring infectious virus titration, showed that TA-Fe^{3+}-MPS as a disinfection modality could be applicable at any climate of cold and hot temperatures between 4 and 37 °C. Taken together, a series of virucidal tests clearly suggested that TA-Fe^{3+}-MPS was able to inactivate respiratory RNA viruses, enveloped or naked, regardless of different temperatures (4 to 37 °C), within 10 min.

Given that most of emerging or re-emerging infectious viral diseases are responsible for zoonoses, it is crucial that their transmission among animals is pre-emptively blocked before they have the ability to spread to humans. Along with the threat to public health, poultry and livestock industries can be immediately devastated by outbreaks of the veterinary or zoonotic viruses, as experienced in the endemics of avian influenza virus, foot-and-mouth disease virus (FMDV), and African swine fever virus. To inactivate the human and animal viruses, chemical disinfectants have widely been used, which are classified into aldehydes, alkali agents, halogen-based compounds, alcohol, peroxide-based compounds, and quaternary ammonium compounds, representatively. Although these materials are highly potent and easily synthesized in a large scale, they have some limitations, such as environmental toxicity facilitating corrosion, extremely short half-life associated with volatility or generation of free radicals, and reduced

activity in the presence of organic materials. In addition, as they are recommended to be stored at above-freezing temperatures, use of these chemical disinfectants would not be possible in extremely cold weather, particularly where avian influenza virus or FMDV circulates readily. Although the disinfectants are stored in optimal conditions, they will become frozen and not sprayable in an outdoor field condition. Our studies provide the empirical evidence demonstrating the broad-spectrum disinfection ability as well as the thermal stability of TA-Fe^{3+}-MPS in both laboratories and daily-life circumstances.

Microbicidal Activity. *E. coli* and *S. typhimurium* were chosen as model pathogenic bacteria to test the bactericidal capability of our spraying system. *E. coli* is one of the most common and widespread pathogens, and is often used as a contamination indicator to assess the quality of water systems. Some strains of *E. coli* are also responsible for foodborne outbreaks, exemplified by the O157 strain that causes severe stomach pain, bloody diarrhoea, and kidney failure. As an instance, the US Department of Agriculture (USDA) recalled nearly 120,900 pounds of ground beef products because of possible contamination with *E. coli* in 2022.[60] *Salmonella* are common but hardy bacteria that can survive several weeks in a dry environment and several months in water.[61] The pathogenic Gram-negative *Salmonella typhimurium*, found in contaminated foods, including eggs, fruits, vegetables, meats, and even processed foods, commonly causes foodborne illness (e.g., food poisoning). In particular, contamination of eggs by *Salmonella* (e.g., *S. typhimurium* and *S. enteritidis*) has calamitous effects on the egg industry.[62,63] To verify the bactericidal activity, *E. coli* were cultured on LB agar plates, followed by the TA-Fe^{3+}-MPS spraying (Figure 3a). The LB agar plates were fully covered after five sprays. It is to note that the one-pot, one-nozzle spraying has not been possible in the conventional MPS formulation because of the rapid precipitation of TA-Fe^{3+} complex in the coating solution.[51] The current method was

based on our own formulation of the MPS that has been demonstrated to be stable in water for a long period of time.[39-42,50] A second *E coli* plate was sprayed with only water as a negative control along with another plate of bacteria without spraying. After 24 h of culture, the CFUs were measured. The CFUs for *E. coli* without spraying were calculated to be 3.3 ± 0.2 log(CFU mL^{-1}), and that for the water-sprayed sample was 3.1 ± 0.2 log(CFU mL^{-1}) (Figure 3b). In stark contrast, no colonies were observed on the plate sprayed with TA-Fe^{3+}-MPS. Similarly, *S. typhimurium* plated on XLD agar showed promising results (Figure 3c). The plate sprayed with the TA-Fe^{3+}-MPS followed by 24 hour culture did not show any growth of *S. typhimurium*, while the plates with no spraying and water-only spraying showed comparable growth, with CFUs of 2.9 ± 0.2 log(CFU mL^{-1}) and 2.4 ± 0.1 log(CFU mL^{-1}), respectively (Figure 3d).

Our spray system was also tested against multidrug resistant *S. aureus* and *A. baumannii* (Table S1). Both bacteria are main agents of nosocomial infections.[64,65] Particularly, bacteria remaining on various surfaces, including catheters and tubing for surgery, create huge problems. Therefore, we investigated whether our spraying system could inhibit the growth of these hospital-infection-related bacteria in the aim of developing a method for disinfecting surfaces in healthcare settings. *S. aureus* (patient-derived USA 300) and *A. baumannii* (patient-derived ATCC 17978) were prepared similarly to *E. coli* or *S. typhimurium* above, except that the TSA plate was used for *S. aureus*. With *S. aureus*, the TA-Fe^{3+}-MPS spray completely inhibited the growth, while the plate of *S. aureus* sprayed with only water or that without spraying showed similar CFUs, 3.7 ± 0.4 log(CFU mL^{-1}) and 4.1 ± 0.3 log(CFU mL^{-1}), respectively (Figure S3a). In contrast, the TA-Fe^{3+}-MPS spray did not show complete inhibition of the *A. baumannii* growth. However, it could be seen that the growth of *A. baumannii* was significantly slowed down. With the TA-Fe^{3+}-MPS spray, CFU was measured to be 2.5 ± 0.6 log(CFU mL^{-1}), while water-sprayed and no-spray

plates showed CFUs of 4.6 ± 0.4 log(CFU mL^{-1}) and 5.1 ± 0.5 log(CFU mL^{-1}), respectively (Figure S3b). These results combined provide proof-of-concept that our spray formulation could be used as a disinfectant against pathogens of critical importance in a healthcare setting.

In addition to pathogenic bacteria, some fungi cause diseases, which can be from merely annoying (e.g., athlete's foot) to life-threatening (e.g., aspergillosis). We investigated the fungicidal activity of the TA-Fe^{3+}-MPS spraying with *P. ostreatus* (oyster mushroom) as a model for safety reasons and easy visualization; *P. ostreatus*, a species of gilled mushrooms, is one of the most commonly cultivated edible mushrooms. The TA-Fe^{3+}-MPS spraying was performed to the mushroom cultivation bottles once a day under ambient conditions, and the mushroom growth was analysed for one week. Water spraying was used as a control. As seen in Figure 4a, in the water-sprayed set, young mushrooms at the button stage were observed after 3 days of cultivation, and thereafter continued to grow rapidly. After 7 days of cultivation they became mature *P. ostreatus* with brown gills (height: 7 cm) (Figure 4b,c). In remarkable contrast, for the TA-Fe^{3+}-MPS-sprayed sample, the little (i.e., small-sized) mushrooms remained at the button stage without growth, and the stalk and head parts were crumpled (i.e., growth inhibition and structure deformation) (Figure 4), indicating the fungicidal activity of our spraying system. The fungicidal activity was additionally demonstrated with *T. rubrum*, which provokes a fungal skin infection known as athlete's foot (tinea pedis). Commercial shoe insoles were immersed in the SD broth solution for 30 min to supply nutrients for colonization, followed by inoculation of *T. rubrum* and incubation for 30 min at ambient temperature. The TA-Fe^{3+}-MPS was then sprayed to the insoles once a day. Control insoles were sprayed with only water. After two days of cultivation, white mould was apparent in the water-sprayed sample, while the growth and spread of *T. rubrum* were suppressed in the TA-Fe^{3+}-MPS-sprayed sample (Figure S4).

Material Independency and Coating Durability. Diverse microorganisms and viruses are present ubiquitously in our living environments, and some cause allergic illnesses and infectious diseases. Accordingly, we examined whether our spraying system could be universally applied to various surfaces, such as glass, metals, ceramics, fabrics, and plastics, by water contact angle analysis. The wettability of various substrates, including AC, Al, Au, Cu, glass, PS, PTFE, Si, Sn, SS, and Ti, was measured before and after TA-Fe^{3+}-MPS spraying (Figure 5a). The contact-angle measurements showed that all of the substrates tested became hydrophilic (contact angle: < 30.4°) after spraying, confirming that the TA-Fe^{3+} films were successfully formed on all of them. The TA-Fe^{3+} films on gold were further characterized, as a representative, by FE-SEM, AFM, XPS, and UV-vis spectroscopy (Figure S5-7). FE-SEM and AFM images showed that the TA-Fe^{3+}-MPS spraying produced flat, uniform films (e.g., root-mean-square roughness: 5.514 nm) (Figure S5), similar to those produced by dip-coating (i.e., MPS assembly).[39] The XPS and UV-vis analyses demonstrated the presence of supramolecular complexes of TA and Fe^{3+} in the films (Figure S6,7). The film thickness could be tuned with ease by changing the molar ratios and concentrations of TA and Fe^{3+} in the MPS preparation (Figure S8). For example, when the TA/Fe^{3+} ratio was fixed to be 1:4, the film thickness could be adjusted from 0 to 50 nm by increasing the concentration of the spraying solution (Figure 5b). In addition to the material independency, we also investigated the coating durability by measuring the L^* (lightness) value in the CIELAB colour space, also known as $L^*a^*b^*$. The L^* is defined as black at 0 and white at 100, and the L^* value of a cotton fabric was measured before and after TA-Fe^{3+}-MPS spraying. After spraying, the white fabric immediately turned dark purple, and the L^* value sharply decreased from 90.4 ± 0.4 to 34.7 ± 1.6, indicating that the TA-Fe^{3+} film was densely formed on the fabric surface (Figure 5c and Figure S9a). No noticeable changes in the L^* value were

observed during the five washing-drying cycles, which clearly demonstrated the durability of the coating. The coating persistence was also observed for chicken eggshells, signifying the disinfecting potential of the TA-Fe^{3+}-MPS spraying for chicken eggs (Figure S9b). Furthermore, the TA-Fe^{3+} films were degradable under eco-friendly, biocompatible conditions. It was confirmed that the films were degraded within 1 min of treatment with ascorbic acid (10 mM) (Figure S10).

Real-Life Setting. For practical real-life applications, we investigated the microbicidal effect of the TA-Fe^{3+}-MPS spraying for various cases in our daily lives, such as air filter membranes, toilet seats, kitchen sinks, refrigerators, disposable face masks, and mobile phones (Figure 6). Samples were collected from each household products and submerged in a 0.85% NaCl solution for 10 min, and a 10-fold diluted solution was applied to the PCA plates. After 30 min of storage under ambient conditions, the TA-Fe^{3+}-MPS spraying was carried out on the PCA plate. All the collected samples, to our surprise, contained microorganisms, and different types of the colonies were observed depending upon the sources (Figure 6a-f). In pleasing contrast, no colonies were observed for all the samples after TA-Fe^{3+}-MPS spraying. As another demonstration, the TA-Fe^{3+}-MPS spraying was applied directly to various items (e.g., toilet seats, kitchen sinks, and mobile phones), and samples were collected from the sprayed surfaces. After 30 h of cultivation, no colonies were detected on the PCA plates (Figure 6g,h). Collectively, these results corroborated that the one-pot TA-Fe^{3+}-MPS spraying effectively deactivates a variety of microorganisms that could pose threats to human health in everyday life.

Long-Term Stability of TA-Fe^{3+}-MPS Solutions. The long-term stability of the spraying solution was studied since degradation (e.g., formation of aggregates) is closely related to the reduction of microbicidal effects as well as product shelf-life. We monitored the evolution of the

TA-Fe^{3+} particles in our TA-Fe^{3+}-MPS spraying solution for 8 weeks with CLSM-DIC mode. The CLSM-DIC images showed that after mixing the TA solution with the Fe^{3+} solution, small particles were formed rapidly within 3 h, but subsequently, the size and number increased extremely slowly over 8 weeks (Figure S11). The average particle size in the scanned area (i.e., 640.17 × 640.17 μm^2) was calculated based on the DIC images. The quantitative data showed a logarithmic growth curve (Figure 7a). For example, the size sharply increased from 0 to 0.04 mm^2 at 3 h of incubation on average, and the size increase slowed down afterwards. No noticeable sediment was observed in the spraying solution during the 8-week monitoring. The TA-Fe^{3+}-MPS spraying produced a 4-nm-thick film after 8 weeks (Figure S12), but it should be noted that the microbicidal ability of the TA-Fe^{3+}-MPS spraying remained unchanged (Figure 7b). For example, the 8-week-old spraying solution completely inactivated the growth of *E. coli* on the LB agar plates (0 log(CFU mL^{-1})), which supported the outstanding long-term stability of our disinfection system.

CONCLUSION

In summary, we have formulated a virucidal and microbicidal spray, composed of nature-derived tannic acid (TA) and iron (Fe^{3+}), for seamless application and implementation to real-life setting. Its disinfection activity shows operational efficacy against a wide range of the pathogens that threaten human health: viruses (influenza viruses, SARS-CoV-2, and human rhinovirus), bacteria (*E. coli* and *S. typhimurium* in the food industry, and *S. aureus* and *A. baumannii* in healthcare setting), and fungi (*P. ostreatus* and *T. rubrum*). This one-pot, one-nozzle spraying system has several advantages. (1) It is extremely simple to use. It requires just the mixing of aqueous TA and Fe^{3+} solutions in a predefined ratio for formulation and spraying onto

contaminated surfaces and areas. Its feasibility with household items (i.e., air filter membranes, toilet seats, kitchen sinks, refrigerators, disposable face masks, and mobile phones) strongly supports the simplicity of its use. (2) It is eco-friendly and would not do any harm to humans, as organic and inorganic composites, TA and Fe^{3+} have been categorised to be generally recognized as safe (GRAS) and approved as food additives by the US FDA. (3) It is cost-effective. The spraying solution can be formulated for less than $3 per litre, which the income level 2 (less than $8000 per year) countries could afford. Moreover, the long-term and thermal stability of the spraying solution would facilitate its practical use. (4) It could serve as an agent for preventive hygiene as well as post-disinfection of contaminated areas, for example as an antimicrobial coating for the filters of air conditioners and cleaners, which is our next research goal.

ASSOCIATED CONTENT

Supporting Information. Inhibition of influenza A virus-induced cytopathic effect by TA-Fe^{3+}-MPS; Inhibition of human rhinovirus-induced cytopathic effect by TA-Fe^{3+}-MPS; Bactericidal effect against *Staphylococcus aureus* and *Acinetobacter baumannii*; Fungicidal effect of TA-Fe^{3+}-MPS spraying against *Trichophyton rubrum*; FE-SEM and AFM images of TA-Fe^{3+} films; Narrow-scanned XPS spectra of TA-Fe^{3+} films; UV-visible absorption spectrum of TA-Fe^{3+} films; Film thicknesses with various concentrations of TA and Fe^{3+}; Photographs of cotton fabric and eggs before and after spraying; Time-lapse DIC images of TA-Fe^{3+} particles; A graph of film thickness versus storage period; Drug resistance profile of bacterial strains.

AUTHOR INFORMATION

Corresponding Authors

Meehyein Kim — Infectious Diseases Therapeutic Research Center, KRICT, Daejeon 34114, Korea; Graduate School of New Drug Discovery and Development, Chungnam National University, Daejeon 34134, Korea; Email: mkim@krict.re.kr

Insung S. Choi — Department of Chemistry, KAIST, Daejeon 34141, Korea; Email: ischoi@kaist.ac.kr

Authors

Sang Yeong Han — Department of Chemistry, KAIST, Daejeon 34141, Korea

Gyeongwon Yun — Department of Chemistry, KAIST, Daejeon 34141, Korea

Hyeon-Min Cha — Infectious Diseases Therapeutic Research Center, KRICT, Daejeon 34114, Korea; Graduate School of New Drug Discovery and Development, Chungnam National University, Daejeon 34134, Korea

Myoung Kyu Lee — Infectious Diseases Therapeutic Research Center, KRICT, Daejeon 34114, Korea

Hojae Lee — Department of Chemistry, Hallym University, Chuncheon 24252, Korea

Eunhye K. Kang — Department of Chemistry, KAIST, Daejeon 34141, Korea

Seok-Pyo Hong — Department of Chemistry, KAIST, Daejeon 34141, Korea

Kirsty A. Teahan — School of Chemistry and Institute for Life Sciences, Highfield Campus, University of Southampton, Southampton SO17 1BJ, United Kingdom

Minjeong Park — Hansol RootOne, Inc., 165 Myeoncheon-ro, Dangjin 31803, Korea

Hansol Hwang — Hansol RootOne, Inc., 165 Myeoncheon-ro, Dangjin 31803, Korea

Seung Seo Lee — School of Chemistry and Institute for Life Sciences, Highfield Campus, University of Southampton, Southampton SO17 1BJ, United Kingdom

Author Contributions

I.S.C., S.Y.H., G.Y. and E.K.K. initiated the project. I.S.C., M.K. and S.S.L. supervised the project. S.Y.H., G.Y. and K.A.T. performed microbicidal and fungicidal studies, and M.K., H.-M.C. and M.K.L. did virucidal studies. E.K.K., S.-P.H, and H.L. formulated the spray solution. E.K.K, M.P. and H.H. performed microbicidal studies on chicken eggs. I.S.C., M.K., K.A.T. and S.S.L. wrote the manuscript with inputs from all authors. ‡S.Y.H. and G.Y. contributed equally.

Notes

The authors declare no competing financial interest.

ACKNOWLEDGMENT

This work was supported by the Basic Science Research Program through the National Research Foundation of Korea (NRF) funded by the Ministry of Science and ICT (MSIT) (2021R1A3A3002527 for I.S.C. and 2018M3A9H4089601 for M.K.). K.A.T. is supported by the Institute for Life Sciences studentship (U. Southampton). Part of the work was supported by Hansol RootOne. The SARS-CoV-2 resource (NCCP No., 43328) was provided by the National Culture Collection for Pathogens, Republic of Korea.

REFERENCES

1. World Health Organization. WHO Coronavirus (COVID-19) Dashboard. https://covid19.who.int.

2. Verschuur, J.; Koks, E. E.; Hall, J. W. Observed Impacts of the COVID-19 Pandemic on Global Trade. *Nat. Hum. Behav.* **2021**, *5*, 305-307.

3. The *Cell* Editorial Team. COVID-19: Navigating Uncertainties Together. *Cell* **2020**, *181*, 209-210.

4. Centers for Disease Control and Prevention. CDC Scientific Brief: SARS-CoV-2 Transmission. https://www.cdc.gov/coronavirus/2019-ncov/science/science-briefs/sars-cov-2-transmission.html.

5. Stadnytskyi, V.; Bax, C. E.; Bax, A.; Anfinrud, P. The Airborne Lifetime of Small Speech Droplets and Their Potential Importance in SARS-CoV-2 Transmission. *Proc. Natl. Acad. Sci. U.S.A.* **2020**, *117*, 11875-11877.

6. Asadi, S.; Wexler, A. S.; Cappa, C. D.; Barreda, S.; Bouvier, N. M.; Ristenpart, W. D. Aerosol Emission and Superemission during Human Speech Increase with Voice Loudness. *Sci. Rep.* **2019**, *9*, 2348.

7. Garcia-Blanco, M. A.; Ooi, E. E.; Sessions, O. M. RNA Viruses, Pandemics and Anticipatory Preparedness. *Viruses* **2022**, *14*, 2176.

8. Wong, K. H.; Lal, S. K. Alternative Antiviral Approaches to Combat Influenza A Virus. *Virus Genes* **2023**, *59*, 25-35.

9. Gilbert, J. A.; Stephens, B. Microbiology of the Built Environment. *Nat. Rev. Microbiol.* **2018**, *16*, 661-670.

10. Chin, A. W. H.; Chu, J. T. S.; Perera, M. R. A.; Hui, K. P. Y.; Yen, H.-L.; Chan, M. C. W.; Peiris, M.; Poon, L. L. M. Stability of SARS-CoV-2 in Different Environmental Conditions. *Lancet Microbe* **2020**, *1*, e10.

11. Gold, K.; Slay, B.; Knackstedt, M.; Gaharwar, A. K. Antimicrobial Activity of Metal and Metal-Oxide Based Nanoparticles. *Adv. Therap.* **2018**, *1*, 1700033.

12. Yang, Y.; Cai, Z.; Huang, Z.; Tang, X.; Zhang, X. Antimicrobial Cationic Polymers: From Structural Design to Functional Control. *Polym. J.* **2018**, *50*, 33-44.

13. Daood, U.; Matinlinna, J. P.; Pichika, M. R.; Mak, K.-K.; Nagendrababu, V.; Fawzy, A. S. A Quaternary Ammonium Silane Antimicrobial Triggers Bacterial Membrane and Biofilm Destruction. *Sci. Rep.* **2020**, *10*, 10970.

14. Ghotaslou, R.; Bahrami, N. Antimicrobial Activity of Chlorhexidine, Peracetic Acid/Peroxide Hydrogen and Alcohol Based Compound on Isolated Bacteria in Madani Heart Hospital, Tabriz, Azerbaijan, Iran. *Adv. Pharm. Bull.* **2012,** *2*, 57-59.

15. Campos, R. K.; Jin, J.; Rafael, G. H.; Zhao, M.; Liao, L.; Simmons, G.; Chu, S.; Weaver, S. C.; Chiu, W.; Cui, Y. Decontamination of SARS-CoV-2 and Other RNA Viruses from N95 Level Meltblown Polypropylene Fabric Using Heat Under Different Humidities. *ACS Nano* **2020**, *14*, 14017-14025.

16. Pullerits, K.; Ahlinder, J.; Holmer, L.; Salomonsson, E.; Öhrman, C.; Jacobsson, K.; Dryselius, R.; Forsman, M.; Paul, C. J.; Rådström, P. Impact of UV Irradiation at Full Scale on Bacterial Communities in Drinking Water. *npj Clean Water* **2020**, *3*, 11.

17. Silindir, M.; Özer, A. Y. Sterilization Methods and the Comparison of E-beam Sterilization with Gamma Radiation Sterilization. *FABAD J. Pharm. Sci.* **2009,** *34*, 43-53.

18. Perelshtein, I.; Lipovsky, A.; Perkas, N.; Gedanken, A.; Moschini, E.; Mantecca, P. The Influence of the Crystalline Nature of Nano-Metal Oxides on Their Antibacterial and Toxicity Properties. *Nano Res.* **2015***, 8*, 695-707.

19. Stensberg, M. C.; Wei, Q.; McLamore, E. S.; Porterfield, D. M.; Wei, A.; Sepúlveda, M. S. Toxicological Studies on Silver Nanoparticles: Challenges and Opportunities in Assessment, Monitoring and Imaging. *Nanomedicine* **2011**, *6*, 879-898.

20. Hora, P. I.; Pati, S. G.; McNamara, P. J.; Arnold, W. A. Increased Use of Quaternary Ammonium Compounds during the SARS-CoV-2 Pandemic and Beyond: Consideration of Environmental Implications. *Environ. Sci. Technol. Lett.* **2020**, *7*, 622-631.

21. Harrell, C. R.; Djonov, V.; Fellabaum, C.; Volarevic, V. Risks of Using Sterilization by Gamma Radiation: The Other Side of the Coin. *Int. J. Med. Sci.* **2018**, *15*, 274-279.

22. Lee, H.; Kim, N.; Rheem, H. B.; Kim, B. J.; Park, J. H.; Choi, I. S. A Decade of Advances in Single-Cell Nanocoating for Mammalian Cells. *Adv. Healthcare Mater.* **2021**, *10*, 2100347.

23. Jia, Z.; Wen, M.; Cheng, Y.; Zheng, Y. Strategic Advances in Spatiotemporal Control of Bioinspired Phenolic Chemistries in Materials Science. *Adv. Funct. Mater.* **2021**, *31*, 2008821.

24. Ejima, H.; Richardson, J. J.; Caruso, F. Metal-Phenolic Networks as a Versatile Platform to Engineer Nanomaterials and Biointerfaces. *Nano Today* **2017**, *12*, 136-148.

25. US Food and Drug Administration. FDA GRAS Substances (SCOGS) Database. https://www.fda.gov/food/generally-recognized-safe-gras/gras-substances-scogs-database.

26. Ekambaram, S. P.; Perumal, S. S.; Balakrishnan, A. Scope of Hydrolysable Tannins as Possible Antimicrobial Agent. *Phytother. Res.* **2016**, *30*, 1035-1045.

27. Sun, H.-q.; Lu, X.-m.; Gao, P.-j. The Exploration of the Antibacterial Mechanism of Fe^{3+} Against Bacteria. *Braz. J. Microbiol.* **2011**, *42*, 410-414.

28. Quideau, S.; Deffieux, D.; Douat-Casassus, C.; Pouységu, L. Plant Polyphenols: Chemical Properties, Biological Activities, and Synthesis. *Angew. Chem. Int. Ed.* **2011**, *50*, 586-621.

29. Stein, J.; Hartmann, F.; Dignass, A. U. Diagnosis and Management of Iron Deficiency Anemia in Patients with IBD. *Nat. Rev. Gastroenterol. Hepatol.* **2010**, *7*, 599-610.

30. Ejima, H.; Richardson, J. J.; Liang, K.; Best, J. P.; van Koeverden, M. P.; Such, G. K.; Cui, J.; Caruso, F. One-Step Assembly of Coordination Complexes for Versatile Film and Particle Engineering. *Science* **2013**, *341*, 154-157.

31. Park, J. H.; Kim, K.; Lee, J.; Choi, J. Y.; Hong, D.; Yang, S. H.; Caruso, F.; Lee, Y.; Choi, I. S. A Cytoprotective and Degradable Metal-Polyphenol Nanoshell for Single-Cell Encapsulation. *Angew. Chem. Int. Ed.* **2014**, *53*, 12420-12425.

32. Park, T.; Kim, J. Y.; Cho, H.; Moon, H. C.; Kim, B. J.; Park, J. H.; Hong, D.; Park, J.; Choi, I. S. Artificial Spores: Immunoprotective Nanocoating of Red Blood Cells with Supramolecular Ferric Ion-Tannic Acid Complex. *Polymers* **2017**, *9*, 140.

33. Park, T.; Kim, W. I.; Kim, B. J.; Lee, H.; Choi, I. S.; Park, J. H.; Cho, W. K. Salt-Induced, Continuous Deposition of Supramolecular Iron(III)-Tannic Acid Complex. *Langmuir* **2018**, *34*, 12318-12323.

34. Lee, J.; Cho, H.; Choi, J.; Kim, D.; Hong, D.; Park, J. H.; Yang, S. H.; Choi, I. S. Chemical Sporulation and Germination: Cytoprotective Nanocoating of Individual Mammalian Cells with a Degradable Tannic Acid-Fe^{III} Complex. *Nanoscale* **2015**, *7*, 18918-18922.

35. Rahim, M. A.; Björnmalm, M.; Bertleff-Zieschang, N.; Besford, Q.; Mettu, S.; Suma, T.; Faria, M.; Caruso, F. Rust-Mediated Continuous Assembly of Metal-Phenolic Networks. *Adv. Mater.* **2017**, *29*, 1606717.

36. Rahim, M. A.; Björnmalm, M.; Bertleff-Zieschang, N.; Ju, Y.; Mettu, S.; Leeming, M. G.; Caruso, F. Multiligand Metal-Phenolic Assembly from Green Tea Infusions. *ACS Appl. Mater. Interfaces* **2018**, *10,* 7632-7639.

37. Kim, B. J.; Han, S.; Lee, K.-B.; Choi, I. S. Biphasic Supramolecular Self-Assembly of Ferric Ions and Tannic Acid across Interfaces for Nanofilm Formation. *Adv. Mater.* **2017**, *29*, 1700784.

38. Maerten, C.; Lopez, L.; Lupattelli, P.; Rydzek, G.; Pronkin, S.; Schaaf, P.; Jierry, L.; Boulmedais, F. Electrotriggered Confined Self-Assembly of Metal-Polyphenol Nanocoatings Using a Morphogenic Approach. *Chem. Mater.* **2017**, *29*, 9668-9679.

39. Yun, G.; Besford, Q. A.; Johnston, S. T.; Richardson, J. J.; Pan, S.; Biviano, M.; Caruso, F. Self-Assembly of Nano- to Macroscopic Metal-Phenolic Materials. *Chem. Mater.* **2018,** *30*, 5750-5758.

40. Yun, G.; Richardson, J. J.; Biviano, M.; Caruso, F. Tuning the Mechanical Behavior of Metal-Phenolic Networks through Building Block Composition. *ACS Appl. Mater. Interfaces* **2019**, *11*, 6404-6410.

41. Yun, G.; Richardson, J. J.; Capelli, M.; Hu, Y.; Besford, Q. A.; Weiss, A. C. G.; Lee, H.; Choi, I. S.; Gibson, B. C.; Reineck, G. P. Caruso, F. The Biomolecular Corona in 2D and Reverse: Patterning Metal-Phenolic Networks on Proteins, Lipids, Nucleic Acids, Polysaccharides, and Fingerprints. *Adv. Funct. Mater.* **2020**, *30*, 1905805.

42. Yun, G.; Kang, D. G.; Rheem, H. B.; Lee, H.; Han, S. Y.; Park, J. H.; Cho, W. K.; Han, S. M. Choi, I. S. Reversed Anionic Hofmeister Effect in Metal-Phenolic-Based Film Formation. *Langmuir* **2020**, *36*, 15552-15557.

43. Lee, H.; Kim, W. I.; Youn, W.; Park, T.; Lee, S.; Kim, T.-S.; Mano, J. F.; Choi, I. S. Iron Gall Ink Revisited: In Situ Oxidation of Fe(II)-Tannin Complex for Fluidic-Interface Engineering. *Adv. Mater.* **2018**, *30*, 1805091.

44. Kim, B. J.; Lee, J. K.; Choi, I. S.; Iron Gall Ink Revisited: Hierarchical Formation of Fe(III)-Tannic Acid Coacervate Particles in Microdroplets for Protein Condensation. *Chem. Commun.* **2019**, *55*, 2142-2145.

45. Zhong, Q.-Z.; Li, S.; Chen, J.; Xie, K.; Pan, S.; Richardson, J. J.; Caruso, F. Oxidation-Mediated Kinetic Strategies for Engineering Metal-Phenolic Networks. *Angew. Chem. Int. Ed.* **2019**, *58*, 12563-12568.

46. Han, S. Y.; Hong, S.-P.; Kang, E. K.; Kim, B. J.; Lee, H.; Kim, W. I.; Choi, I. S. Iron Gall Ink Revisited: Natural Formulation for Black Hair-Dyeing. *Cosmetics* **2019**, *6*, 23.

47. Lee, H.; Park, J.; Han, S. Y.; Han, S.; Youn, W.; Choi, H.; Yun, G.; Choi, I. S. Ascorbic Acid-Mediated Reductive Disassembly of Fe^{3+}-Tannic Acid Shells in Degradable Single-Cell Nanoencapsulation. *Chem. Commun.* **2020**, *56*, 13748-13751.

48. Han, S. Y.; Kang, E. K.; Choi, I. S. Iron Gall Ink Revisited: A Surfactant-Free Emulsion Technology for Black Hair-Dyeing Formulation. *Cosmetics* **2021**, *8*, 9.

49. Lee, H.; Nguyen, D. T.; Kim, N.; Han, S. Y.; Hong, Y. J.; Yun, G.; Kim, B. J.; Choi, I. S. Enzyme-Mediated Kinetic Control of Fe^{3+}-Tannic Acid Complexation for Interface Engineering. *ACS Appl. Mater. Interfaces* **2021**, *13*, 52385-52394.

50. Yun, G.; Youn, W.; Lee, H.; Han, S. Y.; Oliveira, M. B.; Cho, H.; Caruso, F.; Mano, J. F.; Choi, I. S. Dynamic Electrophoretic Assembly of Metal-Phenolic Films: Accelerated Formation and Cytocompatible Detachment. *Chem. Mater.* **2020**, *32*, 7746-7753.

51. Park, J. H.; Choi, S.; Moon, H. C.; Seo, H.; Kim, J. Y.; Hong, S.-P.; Lee, B. S.; Kang, E.; Lee, J.; Ryu, D. H.; Choi, I. S. Antimicrobial Spray Nanocoating of Supramolecular Fe(III)-Tannic Acid Metal-Organic Coordination Complex: Applications to Shoe Insoles and Fruits. *Sci. Rep.* **2017**, *7*, 6980.

52. Zhong, Q.-Z.; Pan, S.; Rahim, M. A.; Yun, G.; Li, J.; Ju, Y.; Lin, Z.; Han, Y.; Ma, Y.; Richardson, J. J.; Caruso, F. Spray Assembly of Metal-Phenolic Networks: Formation, Growth, and Applications. *ACS Appl. Mater. Interfaces* **2018**, *10*, 33721-33729.

53. Kim, H. K.; Kim, H.; Lee, M. K.; Choi, W. H.; Jang, Y.; Shin, J. S.; Park, J.-Y.; Bae, D. H.; Hyun, S.-I.; Kim, K. H.; Han, H. W.; Lim, B.; Choi, G.; Kim, M.; Lim, Y. C.; Yoo, J. Generation of Human Tonsil Epithelial Organoids as an *ex vivo* Model for SARS-CoV-2 Infection. *Biomaterials* **2022**, *283*, 121460.

54. Reed, L. J.; Muench, H. A Simple Method of Estimating Fifty Percent Endpoints. *Am. J. Epidemiol.* **1938**, *27*, 493-497.

55. Coultas, J. A.; Cafferkey, J.; Mallia, P.; Johnston, S. L. Experimental Antiviral Therapeutic Studies for Human Rhinovirus Infections. *J. Exp. Pharmacol.* **2021**, *13*, 645-659.

56. Vasickova, P.; Pavlik, I.; Verani, M.; Carducci, A. Issues Concerning Survival of Viruses on Surfaces. *Food Environ. Virol.* **2010**, *2*, 24-34.

57. Firquet, S.; Beaujard, S.; Lobert, P.-E.; Sané, F.; Caloone, D.; Izard, D.; Hober, D. Survival of Enveloped and Non-Enveloped Viruses on Inanimate Surfaces. *Microbes Environ.* **2015**, *30*, 140-144 (2015).

58. Macinga, D. R.; Sattar, S. A.; Jaykus, L.-A.; Arbogast, J. W. Improved Inactivation of Nonenveloped Enteric Viruses and Their Surrogates by a Novel Alcohol-Based Hand Sanitizer. *Appl. Environ. Microbiol.* **2008**, *74*, 5047-5052.

59. Lin, Q.; Lim, J. Y. C.; Xue, K.; Yew, P. Y. M.; Owh, C.; Chee, P. L.; Loh, X. J. Sanitizing Agents for Virus Inactivation and Disinfection. *VIEW* **2020**, *1*, e16.

60. Coveny, T. Lakeside Refrigerated Services Recalls Ground Beef For E. Coli O103 Concern. *Food Poisoning News* https://www.foodpoisoningnews.com/lakeside-refrigerated-services-recalls-ground-beef-for-e-coli-o103-concern.

61. World Health Organization. Salmonella (non-typhoidal). https://www.who.int/news-room/fact-sheets/detail/salmonella-(non-typhoidal).

62. Gast, R. K.; Jones, D. R.; Guraya, R.; Anderson, K. E.; Karcher, D. M. Contamination of Eggs by *Salmonella Enteritidis* and *Salmonella Typhimurium* in Experimentally Infected Laying Hens in Indoor Cage-Free Housing. *Poult. Sci.* **2021**, *100*, 101438.

63. Gole, V. C.; Torok, V.; Sexton, M.; Caraguel, C. G. B.; Chousalkar, K. K. Association Between Indoor Environmental Contamination by *Salmonella Enterica* and Contamination of Eggs on Layer Farms. *J. Clin. Microbiol.* **2014**, *52*, 3250-3258.

64. Pannewick, B.; Baier, C.; Schwab, F.; Vonberg, R.-P. Infection Control Measures in Nosocomial MRSA Outbreaks—Results of a Systematic Analysis. *PLoS One* **2021**, *16*, e0249837 (2021).

65. Borges Duarte, D. F.; Gonçalves Rodrigues, A. *Acinetobacter baumannii*: Insights towards a Comprehensive Approach for the Prevention of Outbreaks in Health-Care Facilities. *APMIS* **2022**, *130*, 330-337.

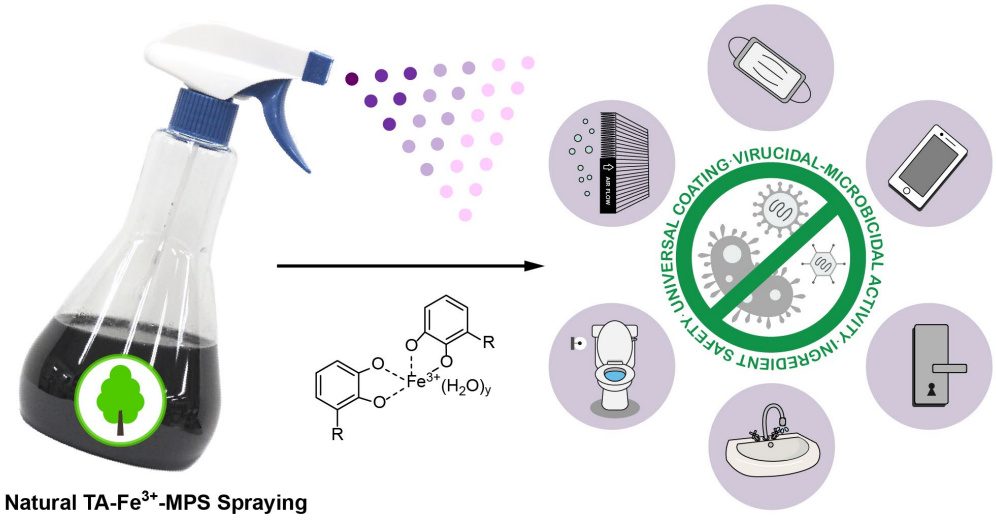

Figure 1. Schematic for natural virucidal and microbicidal TA-Fe^{3+}-MPS spraying against various viruses and microorganisms (potentially) present in our daily lives.

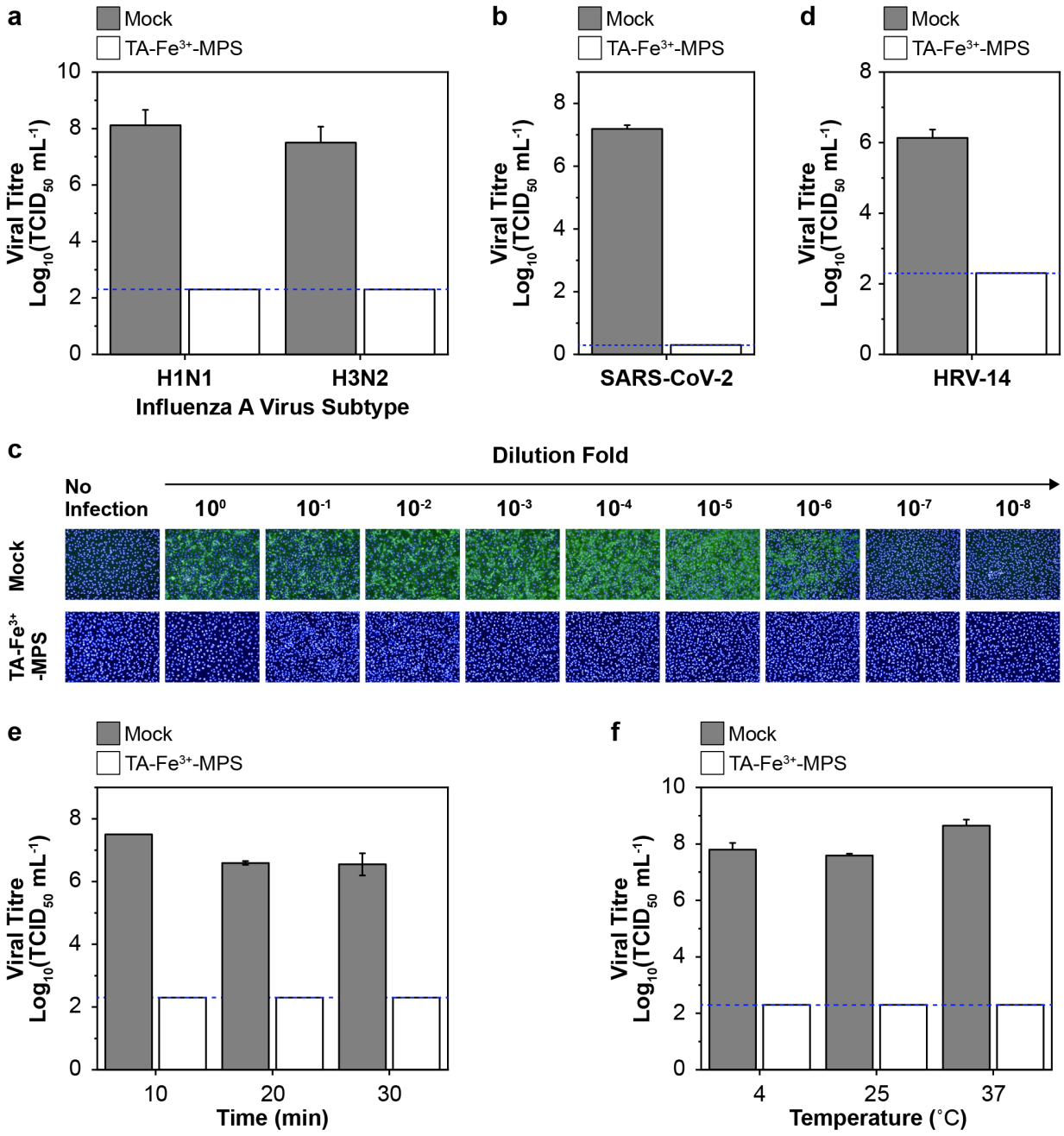

Figure 2. Virucidal effect of TA-Fe^{3+}-MPS against diverse human respiratory viruses. (a) Inactivation of two different subtypes of influenza A virus, H1N1 (A/Puerto Rico/8/34; PR8) and H3N2 (A/Hong Kong/8/68; HK), by TA-Fe^{3+}-MPS. Viral titre was determined by crystal violet staining on day 3 after infection of MDCK cells with each virus mock-treated (Mock) or treated with TA-Fe^{3+}-MPS for 30 min at room temperature. (b) Inactivation of SARS-CoV-2 by TA-

Fe^{3+}-MPS. The virus was treated with mock or TA-Fe^{3+}-MPS at the same condition mentioned in (a). On day 2 after infection of Vero 81 cells, viral S protein was quantified by immunofluorescence assay. (c) Representative immunofluorescent images of (b). Viral S proteins (green) is visualized by staining with its primary antibody and Alexa Fluor 488-conjugated secondary antibody, while nuclei (blue) were counter-stained with DAPI. Original magnification, ×200. (d) Inactivation of human rhinovirus (HRV-14) by TA-Fe^{3+}-MPS. Viral titre was determined using H1 HeLa cells by cytopathic effect assay as mentioned in (a). (e) Time course study on the virucidal effect. Influenza A virus (H1N1; PR8) was mock-treated (Mock) or treated with TA-Fe^{3+}-MPS at room temperature for 10, 20, and 30 min. (f) Temperature-dependency study on the virucidal effect. Influenza A virus (H1N1; PR8) was mock-treated (Mock) or treated with TA-Fe^{3+}-MPS at different temperatures, 4, 25, and 37 °C, for 30 min. Limit of detection (LOD) is marked with blue dashed lines. Data are represented with mean ± SEM from three independent experiments.

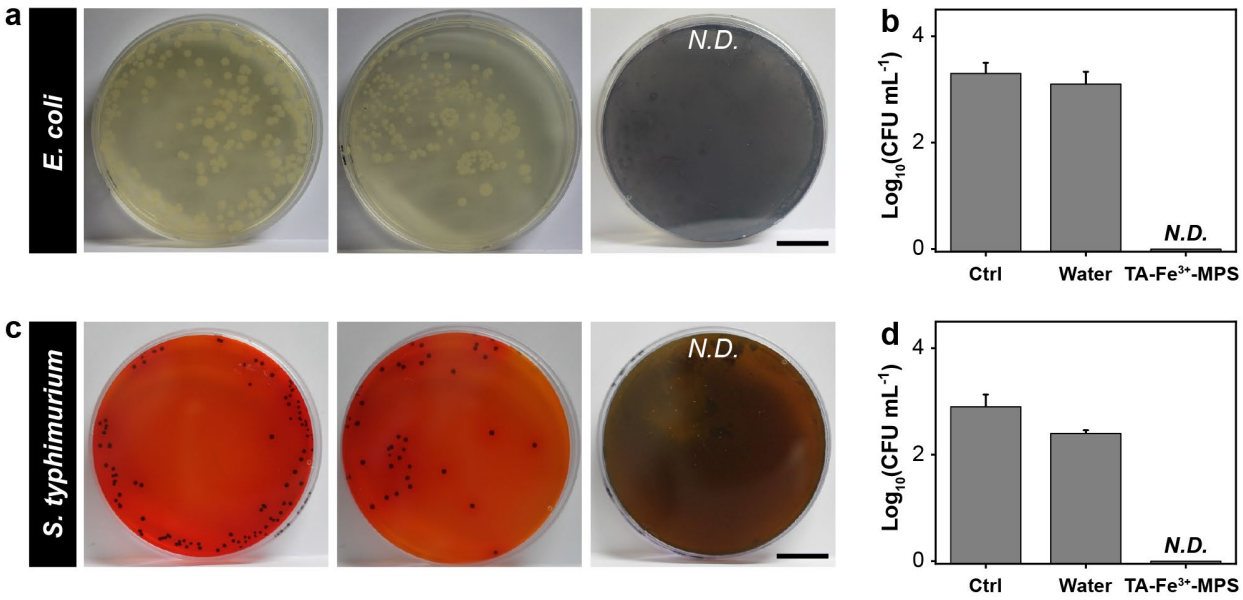

Figure 3. Bactericidal effect against *E. coli* and *S. typhimurium*. (a) Photographs of the agar plates that contain *E. coli* Left: no spraying; middle: water spraying; right: TA-Fe^{3+}-MPS spraying. Scale bar: 2 cm. (b) CFU values of *E. coli*. Ctrl: no spraying; water: water spraying; TA-Fe^{3+}-MPS: TA-Fe^{3+}-MPS spraying; *N.D.*: not detected. (c) Photographs of the agar plates that contain *S. typhimurium.* Left: no spraying; middle: water spraying; right: TA-Fe^{3+}-MPS spraying. Scale bar: 2 cm. (d) CFU values of *S. typhimurium*. Ctrl: no spraying; water: water spraying; TA-Fe^{3+}-MPS: TA-Fe^{3+}-MPS spraying; *N.D.*: not detected. Data are represented as mean ± SD.

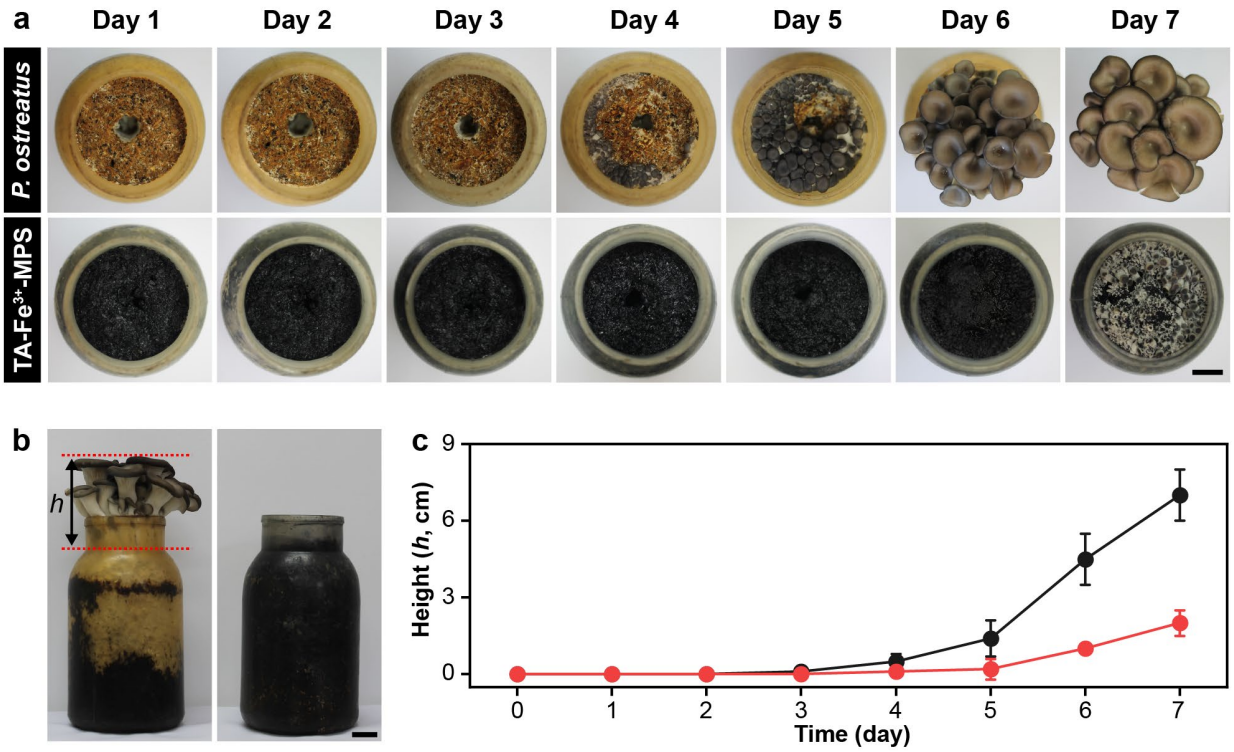

Figure 4. Fungicidal effect against *P. ostreatus*. (a) Photographs of *P. ostreatus* growth from Day 1 to Day 7 (from left to right). Top: water spraying; bottom: TA-Fe^{3+}-MPS spraying. (b) Photographs of *P. ostreatus* at Day 7. Left: water spraying; right: TA-Fe^{3+}-MPS spraying. (c) Graph of *P. ostreatus* growth versus cultivation time. Black: water spraying; red: TA-Fe^{3+}-MPS spraying. Scale bar: 2 cm. Data are represented as mean ± SD.

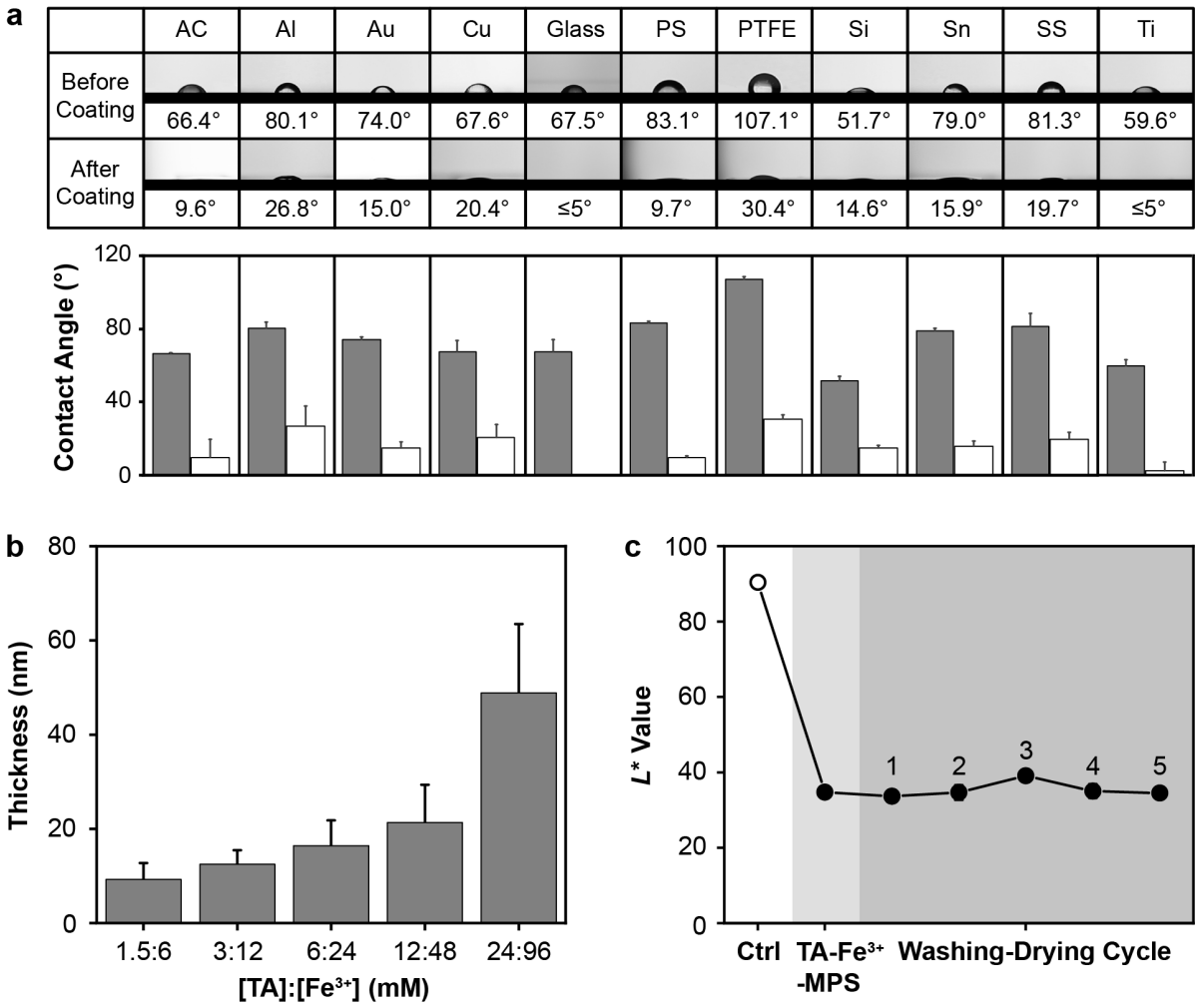

Figure 5. Materials independency and durability of TA-Fe^{3+} coating. (a) Material-independent characteristics of the TA-Fe^{3+} coating. Top: photographs of water droplets on various substrates before and after TA-Fe^{3+}-MPS spraying. Bottom: graph of water contact angles before and after spraying. AC: poly(acrylic acid); Al: aluminium; Au: gold; Cu: copper; PS: polystyrene; PTFE: polytetrafluoroethylene; Si: silicon; Sn: tin; SS: stainless steel; Ti: titanium. (b) Film thickness on gold with various concentrations of TA and Fe^{3+} ([TA]:[Fe^{3+}] = 1:4). (c) Graph of L^* values for repeated washing-drying cycles. Ctrl: no spraying; TA-Fe^{3+}-MPS: TA-Fe^{3+}-MPS spraying. Data are represented as mean ± SD.

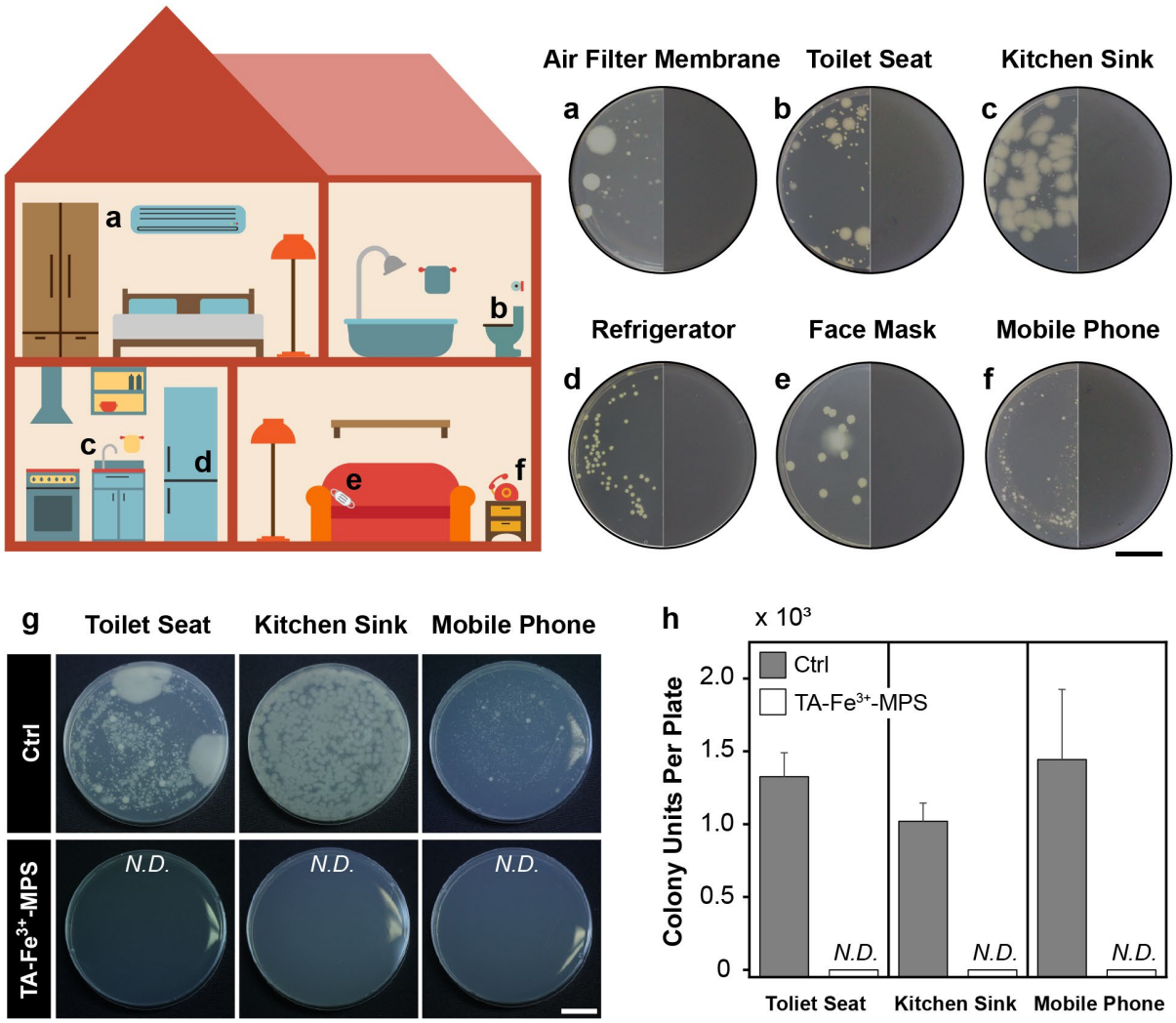

Figure 6. Practical real-life applications. (a-f) Microbicidal activity of the microbicidal spraying against the microorganisms collected from (a) air filter membrane, (b) toilet seat, (c) kitchen sink, (d) refrigerator, (e) face mask, and (f) mobile phone. Left: no spraying; right: microbicidal spraying. (g,h) Real-life applications of the microbicidal spraying on household products. The spraying is done directly onto a toilet seat, a kitchen sink, and a mobile phone, and the samples are collected for CFU analysis. Ctrl: no spraying; TA-Fe^{3+}-MPS: TA-Fe^{3+}-MPS spraying; *N.D.*: not detected. Scale bar: 2 cm. Data are represented as mean ± SD.

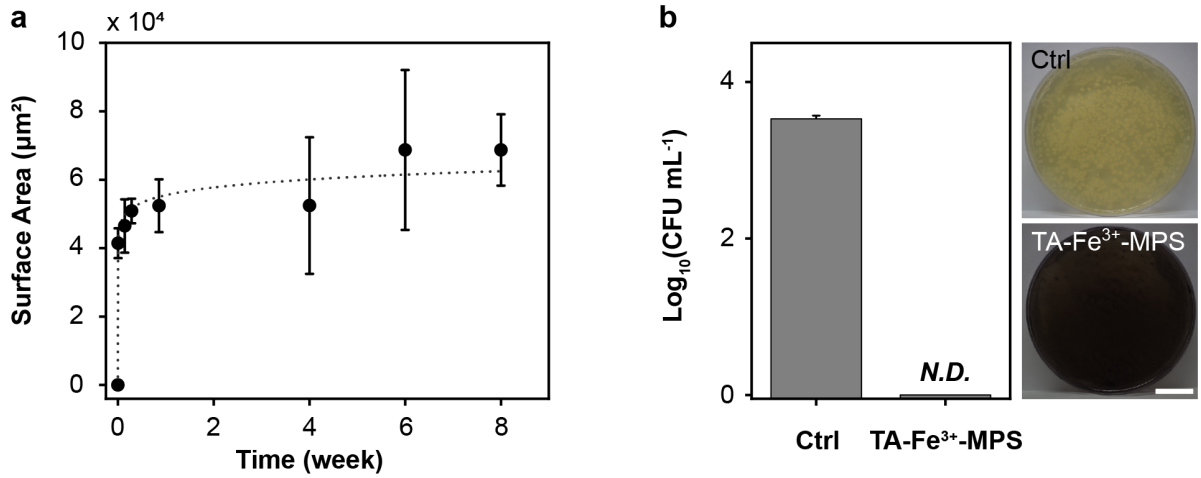

Figure 7. Long-term stability of the microbicidal spraying solution. (a) Graph of the averaged surface area of TA-Fe^{3+} particles in the spraying solution versus time. (b) Bactericidal activity of the 8-week-old spraying solution. Ctrl: no spraying; TA-Fe^{3+}-MPS: TA-Fe^{3+}-MPS spraying; *N.D.*: not detected. Scale bar: 2 cm. Data are represented as mean ± SD.